

1 **Gyenosides modulate NCX calcium flux, insulin secretion and cytoprotection**
2 **in BRIN-BD11 pancreatic β -cells**

3

4 *Chinmai Patibandla*¹, *Xinhua Shu*¹, *Angus M Shaw*¹, *Sharron Dolan*¹
5 *and Steven Patterson*^{1*}

6

7 ^a Department of Biological and Biomedical Sciences, School of Health and Life
8 Sciences, Glasgow Caledonian University, Cowcaddens road, Glasgow, G4 0BA.

9 *** Corresponding author:**

10 Steven Patterson PhD,
11 Department of Biological and Biomedical Sciences,
12 School of Health and Life Sciences,
13 Glasgow Caledonian University,
14 Cowcaddens road,
15 Glasgow, G4 0BA.
16 Tel.: +44 1413313156
17 E-mail Address: Steven.Patterson@gcu.ac.uk

18 **Abstract**

19 Gypenosides are saponins extracted from the plant *Gynostemma pentaphyllum*,
20 suggested to have antidiabetic and anti-obesity potential. However, its mechanism of
21 action is not fully understood. The present study aimed to investigate the
22 cytoprotective and insulin stimulatory effects of gypenosides using the rat BRIN-
23 BD11 β -cell line. Gypenosides provided a significant cytoprotective effect against
24 palmitate-, peroxide- and cytokine-induced cytotoxicity, with upregulation of
25 antioxidant genes *Nrf2*, *Cat*, *Sod1*, and *Gpx1*. Acutely, gypenosides enhanced
26 intracellular calcium ($[Ca^{2+}]_i$) and insulin secretion in a dose-dependent manner. The
27 presence of the sodium/calcium exchanger (NCX) reverse mode inhibitor SN-6
28 blocked the gypenosides mediated increase in $[Ca^{2+}]_i$ but not the insulin secretion.
29 These findings indicate that gypenosides may enhance $[Ca^{2+}]_i$ by activating the
30 reverse mode of NCX channels and a possible calcium-independent mechanism
31 involved in their insulin secretion. Gypenosides also upregulate the antioxidant gene
32 expression and protect against oxidative stress and lipotoxicity, providing the
33 rationale for their observed antidiabetic actions.

34 **Keywords:** Gypenosides, NCX, Cytoprotection, β -cells, insulin

35 **Abbreviations:** Intracellular calcium $[Ca^{2+}]_i$; GYP, Gypenosides; GSIS, Glucose-
36 stimulated insulin secretion;

37 **Introduction**

38 Type 2 diabetes mellitus (T2DM) is a metabolic disorder characterised by reduced
39 peripheral insulin sensitivity, β -cell stress, and dysfunction. This ultimately leads to
40 reduced functional β -cell mass, increasing glucose intolerance, and resultant
41 hyperglycemia. Glucose-stimulated insulin secretion (GSIS) requires glucose
42 metabolism and mitochondrial ATP production. The increase in the ATP/ADP ratio
43 causes closure of ATP-sensitive K^+ channels, membrane depolarisation, the opening
44 of voltage-gated Ca^{2+} channels, and increasing intracellular Ca^{2+} levels, which drives
45 insulin exocytosis (Fu et al., 2013). GSIS also results in the production of reactive
46 oxygen species (ROS) as a by-product during mitochondrial metabolism of glucose
47 in the β -cell. However, these ROS are rapidly converted to less toxic molecules by
48 antioxidant enzymes (Brookes et al., 2004). Prolonged insulin hypersecretion by β -
49 cells to compensate for peripheral insulin resistance causes intracellular ROS
50 accumulation in β -cells. Due to the very low expression of antioxidant enzymes in the
51 β -cells, combined with accumulating ROS, β -cells are susceptible to endoplasmic
52 reticulum stress, initiating proinflammatory responses and eventually causing β -cell
53 apoptosis (Donath et al., 2009). In *in vivo* and *in vitro* studies, activation of *Nrf2* (a
54 master regulator of antioxidant pathways) triggered β -cell self-repair and protected
55 against oxidative stress (Abebe et al., 2017; Bhakkiyalakshmi et al., 2014). Thus,
56 any insulin secretagogue with β -cell protective effects against ROS may have
57 therapeutic potential in T2DM.

58 GYP are dammarane type triterpene glycosides extracted from *Gynostemma*
59 *pentaphyllum* (GP), which structurally resembles ginsenosides of *Panax ginseng*
60 (Bai et al., 2010). GYP has previously shown to have anti-hyperglycaemic and hypo-
61 lipidaemic properties in Zucker fatty rats (Megalli et al., 2006). The herbal extract of

62 GP also reduced hepatic glucose output and enhanced insulin secretion in diabetic
63 Goto-Kakizaki rats (Lokman et al., 2015; Yassin et al., 2011). In T2DM patients, GP
64 tea consumption enhanced insulin sensitivity when taken on its own or in
65 combination with sulfonylureas (Huyen et al., 2012, 2013). Furthermore, in isolated
66 pancreatic islets from healthy Wistar rats and spontaneously diabetic Goto-Kakizaki
67 rats, Phanoside (a GYP extracted from GP) enhanced insulin secretion at both low
68 (3.3mM) and high (16.7mM) glucose concentrations (Hoa et al., 2007).

69 In β -cells, intracellular calcium plays a significant role as a secondary messenger
70 promoting insulin granule docking and fusion with the plasma membrane and release
71 of insulin by exocytosis (Newsholme et al., 2012). There are many calcium channels
72 expressed in β -cells, including L-type, T-type, P/Q type, store-operated calcium
73 channels (SOCC), and sodium-calcium exchanger (NCX). Previous attempts to find
74 the calcium channels involved in GYP-induced insulin secretion were inconclusive
75 (Lokman et al., 2015). In streptozotocin-induced diabetic rats, GYP showed
76 antidiabetic effect by stimulating insulin secretion, reducing glucose and lipid levels,
77 enhancing *Nrf2* and its associated antioxidant gene expression (Gao et al., 2016). A
78 similar *Nrf2* mediated protective effect of GYP was also reported in PC12 cells
79 (neural differentiation cell model) and ARPE19 (retinal pigmental epithelial cells)
80 cells (Alhasani et al., 2018; Meng et al., 2014).

81 The current study focused on elucidating the effects of GYP on insulin secretion and
82 β -cell function, Ca^{2+} signaling, and cytoprotection in the rat clonal BRIN-BD11 β -cell
83 model.

84 **Methods:**

85 **Gyenoside extract preparation:** Gyenosides were purchased from Xi'an Jiatian
86 Biotech Co. Ltd, China (purity 98%). Gyenosides were dissolved in absolute
87 ethanol (25mg/ml) by continuous shaking at room temperature overnight. The
88 extract was sterile filtered through a 0.2µm filter and stored at -20°C until use.

89 **Solutions and Chemicals:** Krebs Ringer bicarbonate buffer (KRBB) was composed
90 of (mmol/L): 115 NaCl, 4.7 KCl, 1.2 KH₂PO₄, 1.2 MgSO₄, 1.28 CaCl₂, 20 HEPES, 24
91 NaHCO₃ and 0.1% (w/v) bovine serum albumin (pH 7.4). Thapsigargin (1138),
92 SKF96365 (1147), and SN-6 (2184) were purchased from Tocris, UK. All other
93 chemicals were from Sigma Aldrich (Poole, UK) unless indicated. For studies with
94 palmitic acid, the palmitic acid was dissolved in 50% ethanol at 70°C and conjugated
95 to 10% (w/v) fatty acid-free BSA in RPMI for 1h at 37°C with constant stirring. The
96 respective palmitic acid stock was diluted 1:10 to give the final concentrations
97 (125µM or 250µM) of palmitate and 1% (w/v) BSA. Final concentrations of ethanol in
98 cell culture medium never exceeded 0.01% (v/v).

99 **BRIN-BD11 cell culture and viability testing:** BRIN-BD11 cells (a kind gift from
100 Prof. Peter Flatt, Ulster University, UK) were cultured in RPMI 1640 medium with
101 2mM L-Glutamine (Lonza, Belgium), supplemented with 10% (v/v) fetal bovine
102 serum (FBS), 50U/ml penicillin/streptomycin and maintained at 37°C with 5% CO₂
103 and 95% air. Cells were trypsinised and sub-cultured at 1:5 dilutions when 80-90%
104 confluence was reached. Passages between 25-40 were used for the experiments.
105 To determine the effects of GYP on cell viability, BRIN-BD11 cells were seeded on
106 96 well plates at 1x10⁴ cells/ well. After overnight culture, cells were incubated with
107 test reagents as indicated in the figures for 6 – 72h and cell viability assessed using
108 MTT assay as described previously (Vasu et al., 2014).

109 **Insulin Secretion studies:** Cells were seeded onto a 12 well tissue culture plate
110 (1.5×10^5 cells/ well) and was incubated overnight in RPMI complete growth
111 medium. For insulin release study, media was removed and cells washed with
112 phosphate-buffered saline (PBS). Cells were preincubated for 40 min in KRBB
113 containing low glucose (1.1mM), prior to replacement with low (1.1 mM) or high
114 glucose (16.7mM) KRBB with or without GYP (1ml/well) and incubated for 1h at
115 37°C. After incubation, test buffer from each well was collected, and insulin levels
116 were estimated using a total rat insulin ELISA kit (Merck Millipore, UK) according to
117 the manufacturer's instructions. An Epoch (BioTek, UK) microplate
118 spectrophotometer was used to read the absorbance at 450nm and 590nm.

119 **Calcium Imaging:** BRIN-BD11 cells were seeded onto glass coverslips (1.0×10^5
120 cells/ coverslip) and allowed to attach overnight in RPMI 1640 complete media.
121 Before use, cells were incubated for 45 min with 2 μ M FURA-2AM (Tocris, UK) in
122 KRBB containing 1.1 mM glucose at 37°C. Coverslips were rinsed with PBS and
123 mounted onto an RC-21BRW closed bath imaging chamber (Warner Instruments)
124 with a P-2 platform. Cells perfused at 1ml/min in low glucose (1.1mM) KRBB for 30
125 min before assessing intracellular calcium. A Nikon Eclipse TE2000-U microscope
126 fitted with Photometrics Cool SNAPTM HQ Camera was used to acquire images. The
127 Fura-2 340/380 ratio was calculated, and graphs plotted using MetaFluor
128 fluorescence ratio imaging software.

129 **Quantitative real-time PCR:** Total RNA was extracted from GYP pre-treated BRIN-
130 BD11 cells using NucleoSpin[®] RNA kit (Macherey-Nagel, UK) according to the
131 manufacturer's protocol. From total RNA, cDNA was synthesised using a High-
132 Capacity cDNA reverse transcription kit (Applied Biosystems, UK). Changes in
133 expression of mRNA levels for genes of interest and reference genes were

134 measured by quantitative real-time PCR using 5X HOT FIREPol® EvaGreen® qPCR
135 Mix Plus (no ROX) (Solis BioDyne, Estonia). Bio-rad CFX96™ Real-Time PCR
136 detection was used for amplification and detection. Cycling conditions used were,
137 95°C for 12min followed by 40 cycles of denaturation (95°C for 15s), annealing (60°C
138 for 20s) and extension (72°C for 20s). At the end of each experiment, melting curve
139 analysis was done to analyse primer specificity.

140 **Western blot:** Cells were lysed with RIPA buffer (150mM NaCl, 0.1% Triton X-100,
141 0.5% Sodium deoxycholate, 0.5% SDS and 50mM Tris-HCl, pH8.0), sonicated and
142 centrifuged to separate any cell debris. Protein concentration in the supernatant was
143 measured using a DC™ Protein assay kit (BIO-RAD, UK) according to the
144 manufacturer's specifications. Proteins were separated by SDS-PAGE and
145 transferred to nitrocellulose membrane using iBlot® blotting system (Thermo
146 Scientific, UK). Membranes were blocked with 5% (w/v) BSA in Tris-buffered saline
147 containing Tween20 for 1h at room temperature and incubated with primary
148 antibodies overnight at 4°C. Primary antibodies and dilutions used were: Anti-
149 Pcsk1 (1:1000) (GTX113797S, Genetex), Anti-Pcsk2 (2µg/ml) (MAB6018-SP, Novus
150 Biologicals), Anti-Pdx1 (1µg/ml) (AF2517, R&D Systems) and Anti-Actin-beta
151 (1:1000) (ab-1801, Abcam UK). Blots were incubated with IRDye® conjugated
152 specific secondary antibodies (1:5000) for 1h at room temperature. Signal was
153 detected using Odyssey® Fc imaging system (LI-COR, UK) and analysed using
154 Image Studio™ software.

155 **Data Analysis:** Results were presented as mean ± S.E.M. Data was analysed using
156 Graphpad PRISM® software (ver 6.01) and unpaired t-test (parametric) for
157 comparing two groups or one-way ANOVA for comparing more than 2 groups with a
158 significance threshold of p<0.05.

159 **Results**

160 **GYP treatment dose-dependently alters BRIN-BD11 cell viability**

161 Concentration-dependent long term (24-72h) effects of GYP on the viability of BRIN-
162 BD11 cells are shown in figure 1. A higher concentration of GYP (100µg/ml) reduced
163 cell viability over 24-72h treatment ($P<0.0001$). GYP at a 50µg/ml concentration over
164 24h treatment showed a slight but significant increase in viability ($P<0.05$). Although
165 at 48h, 50µg/ml showed no significant effect, longer-term treatment (72h)
166 significantly reduced the viability of the cells ($P<0.0001$). Low concentrations of GYP
167 (25-6.25µg/ml) had no significant effect until 48h treatment, where 25 and 12.5µg/ml
168 GYP treatment significantly enhanced cell viability by 1.17- and 1.33-fold ($P<0.05$ &
169 $P<0.01$, respectively). At 72h treatment, 1.9, 1.7- and 1.6-fold increases in viability
170 were observed when treated with 25, 12.5, and 6.25 µg/ml GYP, respectively
171 ($P<0.0001$). As a low concentration of 12.5µg/ml GYP enhanced cell viability
172 significantly at 48 and 72h (1.33 and 1.6-fold respectively), this concentration was
173 used for further testing of GYP's potential protective effects against cytotoxic
174 concentrations of palmitate, peroxide, and a cytokine cocktail. Acute (1 - 6 h)
175 exposure of cells to all GYP concentrations tested did not reduce cell viability (data
176 not shown).

177

178 **GYP has cytoprotective effects against palmitate-, peroxide- and cytokine-** 179 **induced toxicity**

180 Effects of low concentrations of GYP (10, 12.5, and 15µg/ml) against 125 and
181 250µM palmitate-induced toxicity are shown in figure 2A. Palmitate treatment for 24h
182 at a concentration of 125 and 250 µM significantly reduced cell viability ($P<0.0001$)
183 by 50% and 70%, respectively. Low concentrations of GYP (10 & 12.5µg/ml) in the

184 presence of 125 μ M palmitate significantly protected cells from the detrimental
185 actions of palmitate ($P < 0.001$ and $P < 0.0001$, respectively). Treatment of BRIN-BD11
186 cells with GYP (10, 12.5, and 15 μ g/ml) along with higher concentrations (250 μ M) of
187 palmitate also significantly reduced the decline in cell viability ($P < 0.001 - 0.0001$).
188 Peroxide treatment for 6h reduced ($P < 0.0001$) cell viability compared to untreated
189 cells (Figure 2B). The addition of GYP (10, 12.5, and 15 μ g/ml) protected the cells
190 ($P < 0.05 - P < 0.0001$) against the detrimental effects of peroxide.
191 Protective effects of GYP over 24h against inflammatory cytokine cocktail-induced
192 toxicity is shown in figure 2C. The cytokine cocktail containing IL-1 β (50U), TNF- α
193 (1000U), and IFN- γ (1000U) reduced cell viability by 61% ($P < 0.0001$) over 24h. GYP
194 co-treatment (6.25, 12.5, and 25 μ g/ml) protected the cells against cytokine-induced
195 toxicity ($P < 0.0001$), with increased viability of 1.1, 1.2, and 1.2-fold, respectively
196 when compared to cytokine cocktail treatment alone.

197

198 **GYP promote insulin secretion from BRIN-BD11 cells irrespective of glucose** 199 **concentration**

200 BRIN-BD11 cells were incubated in KRBB containing either low (1.1mM) glucose or
201 high (16.7mM) glucose with different concentrations of GYP (6.25, 12.5, 25, 50, and
202 100 μ g/ml) for 1h, and insulin was measured by ELISA (figure 3). High glucose
203 (16.7mM) significantly increased insulin secretion ($P < 0.05$) compared to low glucose.
204 Low concentrations of GYP (6.25, 12.5, and 25 μ g/ml) had no insulin release effects
205 at both low and high glucose. However, GYP at 50 μ g/ml increased insulin release
206 1.9-fold compared to 1.1mM glucose alone ($P < 0.01$) but had no effect at high
207 glucose. GYP at 100 μ g/ml enhanced insulin secretion 4.4-fold ($P < 0.0001$) at 1.1mM
208 glucose and 3-fold ($P < 0.001$) at 16.7mM glucose compared to respective controls.

209 This was similar to secretion in the presence of 10mM L-alanine with increases in
210 insulin secretion of 5- ($P<0.0001$) and 3- ($P<0.0001$) fold at basal and high glucose,
211 respectively.

212 **NCX channels are involved in GYP induced Ca^{2+} uptake but not in insulin** 213 **secretion**

214 Acutely, GYP (50 & 100 μ g/ml) enhances BRIN-BD11 cell [Ca^{2+}]_i levels at both low
215 (1.1mM) and high glucose (16.7mM) which is consistent with GYP ability to enhance
216 insulin secretion (Figure 4A & 4B). To determine the effect of GYP on intracellular
217 stores, ER stores were emptied by the addition of 300nM thapsigargin followed by
218 100 μ g/ml GYP treatment along with the thapsigargin. As expected, thapsigargin
219 significantly increased [Ca^{2+}]_c while the addition of GYP with thapsigargin further
220 enhanced [Ca^{2+}]_i levels, indicating GYP-induced extracellular calcium entry through
221 plasma membrane-bound calcium channels (Figure 4C). Verapamil and mibefradil,
222 L-type and T-type calcium channel blockers, respectively, were used to establish if
223 GYP acted via these channels. GYP-induced Ca^{2+} uptake was unchanged in the
224 presence of either 10 μ M verapamil or 10 μ M mibefradil (Figure 4D&4E). To
225 determine whether store-operated calcium channels (SOCC) are involved in GYP
226 action, BRIN-BD11 cells were incubated with 30 μ M SOCC blocker SKF96365 along
227 with 100 μ g/ml GYP. The presence of SOCC blocker delayed the time to response for
228 GYP but did not block the Ca^{2+} entry induced by GYP (Figure 4F). SN-6 is an NCX
229 reverse mode inhibitor that specifically blocks calcium entry through NCX. Perfusion
230 of BRIN-BD11 cells with GYP (100 μ g/ml) in the presence of 10 μ M SN-6 completely
231 blocked Ca^{2+} entry (Figure 4G), indicating NCX reverse mode activity might be
232 involved in GYP-induced calcium responses. To further investigate if NCX mediated
233 Ca^{2+} entry is involved in Insulin secretory properties of GYP, Insulin secretion was

234 measured with GYP treatment in the presence of SN-6. The presence of SN-6 did
235 not alter the insulin secretion by GYP (Figure 4H) at low glucose concentration,
236 indicating Ca²⁺ independent pathways might be involved in the GYP mechanism.

237 **Treatment with GYP changes BRIN-BD11 gene expression**

238 Following 24h treatment with GYP (12.5µg/ml), the expression of antioxidant genes
239 *Sod1* (P<0.01) and *Cat* (P<0.05) were increased, while *Gpx1* expression was
240 unchanged and *Ho1* expression was downregulated (P<0.0001) (Figure 5A).
241 Interestingly, 72h treatment significantly increased expression of all antioxidant
242 genes (*Sod1* (P<0.05), *Cat* (P<0.001), *Gpx1* (P<0.001), *Ho1* (P<0.001). However, no
243 change in *Sod2* expression was observed at any time point.

244 As *Nrf2* regulates the expression of antioxidant genes, changes in expression of *Nrf2*
245 along with its regulator, *Keap1*, were investigated following 24 & 72h GYP treatment.
246 GYP treatment for 24h did not affect *Nrf2* and *Keap1* expression, while 72h
247 treatment resulted in significant increases in both *Nrf2* and *Keap1* (P<0.01) (Figure
248 5B). *Nfkb* mediates cytokine-induced toxicity in β-cells, and as GYP treatment
249 protected against cytokine-induced toxicity, changes in *Nfkb1* & *Nfkb2* were
250 investigated. Both *Nfkb1* & *Nfkb2* expression was downregulated (P<0.0001) by
251 GYP after 24h. However, unexpectedly a significant (P<0.05) increase in expression
252 of both genes was observed following 72h GYP culture (Figure 5B).

253 Treatment with GYP for 24h enhanced *Erk1* expression (P<0.001) while *Erk2*
254 (P<0.01), *Jnk1* (P<0.01), *cJun* (P<0.0001), and *cMyc* (P<0.0001) expression were
255 downregulated (Figure 5C). At 72h, *Erk2* and *Jnk1* expression were unchanged,
256 while *Erk1*, *cJun*, and *Myc* expression were upregulated (P<0.01, P<0.001 &
257 P<0.001, respectively) (Figure 5C).

258 Expression of key β -cell genes, *Ins1* and *Pdx1*, increased significantly ($P < 0.01$ and
259 $P < 0.05$, respectively) following 24h GYP treatment (Figure 5D), while glucokinase
260 (*Gck*) and *MafA* expression were unchanged. Following 72h treatment of BRIN-
261 BD11 with GYP *Ins1* expression was still raised ($P < 0.05$), however, *Pdx1* and *Gck*
262 expression were decreased ($P < 0.0001$), and *MafA* expression remained unchanged
263 (Figure 5D).

264 *Pde4b*, associated with cAMP degradation, was downregulated following 24h GYP
265 treatment ($P < 0.01$), although *Pde3b* expression was unchanged. Both *Pde4b* and
266 *Pde3b* were significantly downregulated at 72h ($P < 0.001$ and $P < 0.01$, respectively)
267 (Figure 5E). Calcium-associated calmodulin (*Calm1*) expression was upregulated
268 ($P < 0.001$) by 24h GYP treatment, while no change in NCX1 expression was
269 observed. Both *Calm1* and NCX1 expression were upregulated following 72h GYP
270 treatment ($P < 0.01$) (Figure 5E).

271 **Long term treatment with GYP reduces the expression of *Pdx1* but not**
272 **Prohormone convertases (*Pcsk1* & *Pcsk2*)**

273 Effects of 24h & 72h culture of BRIN-BD11 cells with GYP on specific changes in
274 critical cellular proteins are shown in figures 6. As GYP treatment altered the
275 expression of genes necessary for insulin production in the β -cells, protein levels of
276 *Pdx1* (necessary for insulin gene transcription), *Pcsk1*, and *Pcsk2* (both necessary
277 for post-translational modification of proinsulin to insulin) were determined by
278 western blot analysis. At 24h, GYP (12.5 μ g/ml) had no significant effect on protein
279 levels of *Pdx1*, while extended treatment for 72h significantly reduced *Pdx1* protein
280 levels (Figure 6 A&B), consistent with changes seen at the mRNA levels shown in
281 figure 5D. Expression of *Pcsk1* and *Pcsk2* were unchanged by GYP treatment.

282 **Discussion**

283 Glucose-stimulated insulin secretion (GSIS) involves ATP-sensitive K^+ channel
284 closure, membrane depolarisation, and increased cytoplasmic calcium levels through
285 the opening of voltage-dependent calcium channels (VDCC), including L-type, T-
286 Type, and P/Q-type Ca^{2+} channels (Yang et al., 2006). The endoplasmic reticulum
287 (ER) acts as an intracellular Ca^{2+} store, and its Ca^{2+} levels are maintained by Sarco-
288 endoplasmic reticulum Ca^{2+} -ATPase (SERCA) pumps. In GSIS, Ca^{2+} is released
289 from ER stores into the cytoplasm along with extracellular Ca^{2+} influx. In the case of
290 ER store Ca^{2+} depletion, store-operated calcium channels (SOCC) bound to the
291 plasma membrane refill the ER and also enhance cytoplasmic Ca^{2+} (R. Wang et al.,
292 2013). The rise in cytoplasmic Ca^{2+} ions, as a secondary messenger, is linked to
293 many functions, including insulin exocytosis. In the current study, we report that GYP
294 enhances $[Ca^{2+}]_i$ and insulin secretion in a concentration-dependent manner at low
295 and high glucose concentrations. These results are consistent with previous results
296 in isolated wild-type and diabetic Goto-kakizaki rat islets, where Phanoside (a
297 Gypenoside) enhanced insulin secretion irrespective of glucose concentration (Hoa
298 et al., 2007). The increase in $[Ca^{2+}]_i$ stimulated by GYP was unaffected by L-type
299 calcium channel blocker verapamil, T-type calcium channel blocker mibefradil, and
300 store-operated calcium channel blocker SKF96365. Thapsigargin is known to
301 deplete the ER store calcium by blocking SERCA-induced calcium uptake into ER
302 stores (Lytton et al., 1991). Thapsigargin induced ER depletion followed by GYP
303 treatment enhanced $[Ca^{2+}]_i$ on top that caused by thapsigargin indicating extracellular
304 calcium mobilisation mediated by plasma membrane-bound channels was key in
305 GYP actions.

306 Plasma membrane Ca^{2+} -ATPase (PMCA) and plasma membrane $\text{Na}^+/\text{Ca}^{2+}$
307 exchanger (NCX) extrude Ca^{2+} ions from the β -cell (Chen et al., 2003). NCX can
308 work in a bidirectional manner; in forward mode, it expels Ca^{2+} and, in reverse mode,
309 increases $[\text{Ca}^{2+}]_i$ (Philipson et al., 2002). It transports 3 Na^+ ions for every Ca^{2+} ion.
310 NCX exists in three isoforms NCX1, NCX2, and NCX3, encoded by genes *Slc8a1-3*.
311 Rat pancreatic β -cells and β -cell models (RINm5F and BRIN-BD11) express two
312 splice variants of NCX1 (NCX1.3 and NCX1.7) (F Van Eylen et al., 1997; Françoise
313 Van Eylen et al., 2002). Benzyloxyphenyl derivatives like KB-R7943, SEA0400, and
314 SN-6 are known for their NCX reverse mode inhibitory effects. Among the three, SN-
315 6 is a potent and selective inhibitor of Ca^{2+} entry through NCX reverse mode
316 (Iwamoto, 2004). We found that, in the presence of SN-6, GYP's ability to stimulate
317 and increase $[\text{Ca}^{2+}]_i$ was completely abolished, indicating GYP interacts with NCX
318 reverse mode mediated Ca^{2+} entry. However, the Presence of SN-6 did not affect the
319 GYP induced insulin secretion, indicating GYP might also promote calcium-
320 independent insulin secretion pathways. It is previously reported that cAMP can
321 potentiate insulin secretion independent of Ca^{2+} (Ämmälä et al., 1993; Kim et al.,
322 2008), which could be the mechanism of GYP.

323 Reduced functional β -cell mass is characteristic of Type 1 diabetes and is also
324 observed in Type 2 diabetes. Apoptosis is one of the significant causes for β -cell loss
325 in T2DM and responsible for its progression (Butler et al., 2003). The contributing
326 factors for β -cell apoptosis include inflammation involving an array of cytokines,
327 oxidative stress caused by ROS/RNS, glucotoxicity due to prolonged hyperglycemia,
328 and hyperlipidemia-induced lipotoxicity. Proinflammatory cytokines, specifically,
329 interleukin 1- β (IL-1 β), interferon γ (IFN- γ) and tumor necrosis factor- α (TNF- α), are
330 linked to β -cell inflammation and apoptosis in Type1 diabetes mellitus (Donath et al.,

331 2003). In T2DM, increased cytokine levels and immune cell infiltration have been
332 observed in the islets, indicating an inflammatory response (Ehnes et al., 2007).
333 Although IL-1 β is produced in the β -cells in response to high glucose, the levels
334 produced are not sufficient to cause apoptosis in purified rat, and human β -cells and
335 combination with IFN- γ are necessary to promote apoptosis (Quan *et al.*, 2013).
336 Exposure of rat and human β -cell models (BRIN-BD11 and 1.1B4) to cytokine
337 cocktail of IL-1 β , IFN- γ , and TNF- α , has previously been demonstrated to cause
338 cellular apoptosis (Kiely et al., 2007; Vasu et al., 2014). Previous studies with GYP
339 have shown anti-inflammatory properties in microglial cells (Cai *et al.*, 2016) and
340 retinal pigment epithelial cells (Alhasani et al., 2018) by reducing cytokine levels. In
341 chondrocytes, GYP was also able to protect against IL-1 β mediated inflammation
342 (Wan et al., 2017). Similar to these results, we have observed a protective effect of
343 GYP in BRIN-BD11 cells against a decline in cell viability caused by a
344 proinflammatory cytokine cocktail of IL-1 β , IFN- γ , and TNF- α . Thus GYP may protect
345 β -cells against inflammatory damage caused by metabolic disarray in obesity and
346 diabetes.

347 Increased circulating free fatty acid (FFA) levels in obesity are one of the risk factors
348 that are linked to the development and progression of type 2 diabetes. Chronic
349 exposure to FFA due to substrate competition results in impaired glucose
350 metabolism and favors FFA oxidation in the β -cell (Lupi et al., 2002). Acutely, FFA
351 can stimulate insulin secretion through $G\alpha_{q/11}$ coupled free fatty acid receptor 1
352 (*FFAR1/GPR40*) (Mancini et al., 2013). However, chronic exposure to elevated levels
353 of FFA is linked to ER stress and β -cell apoptosis (Oh et al., 2018). Saturated FFA
354 like palmitate is known to reduce GSIS and increase β -cell apoptosis in both human
355 and rat models (Karaskov et al., 2006; Lupi et al., 2002). In primary hepatocytes,

356 gypenoside treatment protected against palmitate-induced cell apoptosis (Müller et
357 al., 2012). In our studies, a similar protective effect against palmitate in BRIN-BD11
358 cells was observed when GYP was added to the cells, further supporting the idea
359 that GYP has broad-ranging beneficial cytoprotective effects in β -cells.

360 ROS (Superoxide O_2^- and hydroxyl radical $[HO\cdot]$) are by-products of the
361 mitochondrial respiratory chain, and their production is linked to mitochondrial
362 metabolism (Drews et al., 2010). Superoxide dismutase (*Sod*) converts reactive O_2^-
363 into less reactive hydrogen peroxide (H_2O_2). Catalase (*Cat*) and glutathione peroxidase
364 (*Gpx*) convert H_2O_2 into oxygen and water. Compared to the liver, expression levels
365 of antioxidant molecules is much lower in pancreatic β -cells, with expression at 50%
366 for *Sod* and only 5% for *Cat* and *Gpx* compared to liver, thus making them very
367 susceptible to oxidative stress-induced damage (Tiedge et al., 1997). It is known that
368 hyperglycemia and hyperlipidemia are linked to the elevation of ROS levels in β -
369 cells. Although GSIS produces ROS via mitochondrial metabolism, chronic
370 hyperglycemia in diabetes is linked to ROS accumulation, loss of mitochondrial
371 membrane potential ($\Delta\psi_m$), and eventually β -cell apoptosis (Sivitz et al., 2010; J.
372 Wang et al., 2017). In our studies, GYP treatment in BRIN-BD11 cells protected
373 against H_2O_2 induced oxidative stress compared to untreated cells. Similar GYP
374 protective effects against H_2O_2 have also been observed previously in retinal
375 pigmental epithelial cells, vascular endothelial cells, and liver microsomes (Alhasani
376 et al., 2018; Li et al., 1993). Thus, in β -cells, GYP may reduce the harmful effects of
377 chronic ROS overproduction under metabolic stress and enhance β -cell function.

378 *Nrf2* is a master regulator of antioxidant gene transcription, which interacts with
379 Kelch-like ECH-associated protein 1 (*Keap1*). Previous studies in db/db mice
380 showed that *Nrf2* activation prevented β -cell oxidative damage and diabetes onset

381 (Yagishita et al., 2014). In female Zucker diabetic rats, the *Nrf2-Keap1* pathway
382 mediated β -cell self-repair after high fat diet-induced oxidative damage (Abebe et al.,
383 2017). In isolated human islets, the *Nrf2* activator, dh404, increased antioxidant
384 enzymes' expression and decreased inflammatory mediators (Masuda et al., 2015).
385 Previous studies in diabetic animal models and cell lines suggest that GYP elicits its
386 cytoprotective effects by enhancing the *Nrf2* signaling pathway (Alhasani et al.,
387 2018; Gao et al., 2016; Meng et al., 2014). In line with these reports, the current
388 study in BRIN-BD11 cells produced a similar upregulation of *Nrf2* expression by GYP
389 and its associated antioxidant genes *Sod1*, *Cat*, *Gpx1*, and *Ho1*. We also noticed a
390 downregulation of *Nfkb1* and *Nfkb2* expression, which is associated with
391 proinflammatory responses. *Erk1* (*Mapk3*) and *Erk2* (*Mapk1*) are dominantly
392 expressed MAPKs in the pancreatic β -cells and are associated with cellular
393 proliferation (Jiang et al., 2018). In rat INS-1 insulinoma cell lines, glucose and GLP-
394 1 induced cell proliferation is linked to Ca^{2+} mediated *ERK1/2* activation (Arnette et
395 al., 2003). In the current study, GYP enhanced *Erk1* mRNA expression at 24 and
396 72h while protein levels of total *Erk1/2* were unchanged (data not shown). It has
397 previously been reported that in INS-1 cells, *Erk1/2* activation occurs within 30mins
398 of exposure to high glucose or forskolin, indicating changes in *Erk1/2* occurs at a
399 much earlier time scale than 24h or 72h, which we have used in the current study
400 (Arnette et al., 2003). This could be the possible reason for unaltered protein levels
401 of total *Erk1/2* by GYP at 24h / 72h.

402 Pancreatic/duodenal homeobox1 (*Pdx1*) and MAF BZIP Transcription Factor A
403 (*MafA*) are the key transcription factors that bind to the insulin gene and promote its
404 transcription. *Pdx1* plays a significant role in the development and function of β -cell,
405 whereas *MafA* is necessary for GSIS (Melloul et al., 2002; Zhang et al., 2005). Post-

406 translational modification of proinsulin by *Pcsk1* and *Pcsk2* produces bioactive
407 insulin and C-peptide. Our findings have shown an increase in *Ins1* expression
408 following GYP treatment, whereas *Pdx1* gene expression and protein level were
409 reduced by 72 h GYP treatment. In contrast, *MafA* expression was unchanged along
410 with *Pcsk1* and *Pcsk2* protein levels. Interestingly, *cMyc* levels are higher in juvenile
411 islets but reduced in adult islets, and high levels of *cMyc* while enhancing β -cell
412 proliferation, cause a decrease in *Pdx1* expression by binding to canonical binding
413 sites upstream of *Pdx1*, but not *MafA* (Puri et al., 2018). This supports the idea that
414 in BRIN-BD11 cells in the current study, GYP, while increasing *cMyc* and increasing
415 cell proliferation, most probably does this at the expense of *Pdx1* expression and β -
416 cell maturity.

417 Calmodulin is a ubiquitous protein associated with calcium-dependent activation of
418 membrane-bound adenylyl cyclases (ACs) (Sharp et al., 1980). These ACs generate
419 cAMP from ATP, and intracellular cAMP levels are further regulated by cyclic
420 nucleotide phosphodiesterase (PDE) mediated degradation into 5'-AMP. cAMP, as a
421 secondary messenger, exerts its functions predominantly through activating PKA,
422 which has multiple cellular functions, including regulation of proliferation through
423 phosphorylation of transcription factors such as *cMyc* (Padmanabhan et al., 2013)
424 and *cJun* (Heinrich et al., 1997), regulation of mitogen-activated protein kinases like
425 *Erk1/2* (Briaud et al., 2003) and *Jnk* (Hur, 2005), regulation of antioxidant response
426 through *Nrf2* (Kulkarni et al., 2014) and anti-inflammatory response by inhibiting *Nfkb*
427 activity (Takahashi et al., 2002). The current study shows that GYP enhances
428 calmodulin (*Calm*) expression and downregulates *Pde3b* and *Pde4b* expression in
429 BRIN-BD11 cells, indicating possible enhanced cAMP levels and perhaps
430 downstream responses. However, cAMP and PKA pathways were not investigated in

431 the current study as previous studies in isolated rat islets reported that GYP effect
432 was mediated through PKA (Lokman et al., 2015). However, our results showed
433 modulation of expression of genes both upstream and downstream of PKA
434 suggesting an involvement of PKA activation in the beneficial effects of GYP in
435 BRIN-BD11 cells.

436 **Conclusion**

437 GYP enhanced Ca^{2+} uptake in BRIN-BD11 cells, which may be mediated by NCX
438 reverse mode activation. GYP also enhanced insulin release irrespective of
439 extracellular glucose concentration and showed cytoprotective effects against
440 saturated free fatty acid palmitate, H_2O_2 , cytokine cocktail, and enhanced antioxidant
441 and pro-proliferative gene expression while downregulating proinflammatory
442 response mediating genes. Further studies are required to confirm these findings in
443 primary β -cells and human islets and to further establish and confirm the potential
444 interaction with NCX channels involved in GYP action.

445 **Acknowledgments:** We would like to thank Prof. Peter Flatt, Ulster University, for
446 his kind gift of BRIN-BD11 cells.

447 **Funding:** This research did not receive any specific grant from funding agencies in
448 the public, commercial, or not-for-profit sectors.

449 **Conflict of interest:** The authors have no conflicts of interest to declare.

450 **References**

- 451 Abebe, T., Mahadevan, J., Bogachus, L., Hahn, S., Black, M., Oseid, E., Urano, F.,
452 Cirulli, V., & Robertson, R. P. (2017). Nrf2/antioxidant pathway mediates β cell
453 self-repair after damage by high-fat diet-induced oxidative stress. *JCI Insight*,
454 2(24), e92854. <https://doi.org/10.1172/jci.insight.92854>
- 455 Alhasani, R. H., Biswas, L., Tohari, A. M., Zhou, X., Reilly, J., He, J.-F., & Shu, X.
456 (2018). Gypenosides protect retinal pigment epithelium cells from oxidative
457 stress. *Food and Chemical Toxicology*, 112, 76–85.
458 <https://doi.org/10.1016/j.fct.2017.12.037>
- 459 Ämmälä, C., Ashcroft, F. M., & Rorsman, P. (1993). Calcium-independent
460 potentiation of insulin release by cyclic AMP in single β -cells. *Nature*, 363(6427),
461 356–358. <https://doi.org/10.1038/363356a0>
- 462 Arnette, D., Gibson, T. B., Lawrence, M. C., January, B., Khoo, S., McGlynn, K.,
463 Vanderbilt, C. A., & Cobb, M. H. (2003). Regulation of ERK1 and ERK2 by
464 glucose and peptide hormones in pancreatic beta cells. *The Journal of*
465 *Biological Chemistry*, 278(35), 32517–32525.
466 <https://doi.org/10.1074/jbc.M301174200>
- 467 Bai, M.-S., Gao, J.-M., Fan, C., Yang, S.-X., Zhang, G., & Zheng, C.-D. (2010).
468 Bioactive dammarane-type triterpenoids derived from the acid hydrolysate of
469 *Gynostemma pentaphyllum* saponins. *Food Chemistry*, 119(1), 306–310.
470 <https://doi.org/10.1016/j.foodchem.2009.06.033>
- 471 Bhakkiyalakshmi, E., Shalini, D., Sekar, T. V., Rajaguru, P., Paulmurugan, R., &
472 Ramkumar, K. M. (2014). Therapeutic potential of pterostilbene against
473 pancreatic beta-cell apoptosis mediated through Nrf2. *British Journal of*
474 *Pharmacology*, 171(7), 1747–1757. <https://doi.org/10.1111/bph.12577>

- 475 Briaud, I., Lingohr, M. K., Dickson, L. M., Wrede, C. E., & Rhodes, C. J. (2003).
476 Differential activation mechanisms of Erk-1/2 and p70(S6K) by glucose in
477 pancreatic beta-cells. *Diabetes*, 52(4), 974–983.
478 <https://doi.org/10.2337/diabetes.52.4.974>
- 479 Brookes, P. S., Yoon, Y., Robotham, J. L., Anders, M. W., & Sheu, S.-S. (2004).
480 Calcium, ATP, and ROS: a mitochondrial love-hate triangle. *American Journal of*
481 *Physiology-Cell Physiology*, 287(4), C817–C833.
482 <https://doi.org/10.1152/ajpcell.00139.2004>
- 483 Butler, A. E., Janson, J., Bonner-Weir, S., Ritzel, R., Rizza, R. A., & Butler, P. C.
484 (2003). Beta-cell deficit and increased beta-cell apoptosis in humans with type 2
485 diabetes. *Diabetes*, 52(1), 102–110. <https://doi.org/10.2337/diabetes.52.1.102>
- 486 Cai, H., Liang, Q., & Ge, G. (2016). Gypenoside Attenuates β Amyloid-Induced
487 Inflammation in N9 Microglial Cells via SOCS1 Signaling. *Neural Plasticity*,
488 2016, 6362707. <https://doi.org/10.1155/2016/6362707>
- 489 Chen, L., Koh, D.-S., & Hille, B. (2003). Dynamics of calcium clearance in mouse
490 pancreatic beta-cells. *Diabetes*, 52(7), 1723–1731.
491 <https://doi.org/10.2337/diabetes.52.7.1723>
- 492 Donath, M. Y., Böni-Schnetzler, M., Ellingsgaard, H., & Ehses, J. A. (2009). Islet
493 inflammation impairs the pancreatic beta-cell in type 2 diabetes. *Physiology*,
494 24(6), 325–331. <https://doi.org/10.1152/physiol.00032.2009>
- 495 Donath, M. Y., Størling, J., Maedler, K., & Mandrup-Poulsen, T. (2003). Inflammatory
496 mediators and islet beta-cell failure: a link between type 1 and type 2 diabetes.
497 *Journal of Molecular Medicine*, 81(8), 455–470. [https://doi.org/10.1007/s00109-](https://doi.org/10.1007/s00109-003-0450-y)
498 003-0450-y
- 499 Drews, G., Krippeit-Drews, P., & Düfer, M. (2010). Oxidative stress and beta-cell

- 500 dysfunction. *European Journal of Physiology*, 460(4), 703–718.
501 <https://doi.org/10.1007/s00424-010-0862-9>
- 502 Ehses, J. A., Perren, A., Eppler, E., Ribaux, P., Pospisilik, J. A., Maor-Cahn, R.,
503 Gueripel, X., Ellingsgaard, H., Schneider, M. K. J., Biollaz, G., Fontana, A.,
504 Reinecke, M., Homo-Delarche, F., & Donath, M. Y. (2007). Increased number of
505 islet-associated macrophages in type 2 diabetes. *Diabetes*, 56(9), 2356–2370.
506 <https://doi.org/10.2337/db06-1650>
- 507 Fu, Z., Gilbert, E. R., & Liu, D. (2013). Regulation of insulin synthesis and secretion
508 and pancreatic Beta-cell dysfunction in diabetes. *Current Diabetes Reviews*,
509 9(1), 25–53. <https://doi.org/10.2174/1573399811309010025>
- 510 Gao, D., Zhao, M., Qi, X., Liu, Y., Li, N., Liu, Z., & Bian, Y. (2016). Hypoglycemic
511 effect of *Gynostemma pentaphyllum* saponins by enhancing the Nrf2 signaling
512 pathway in STZ-inducing diabetic rats. *Archives of Pharmacal Research*, 39(2),
513 221–230. <https://doi.org/10.1007/s12272-014-0441-2>
- 514 Heinrich, R., & Kraiem, Z. (1997). The protein kinase A pathway inhibits c-jun and c-
515 fos protooncogene expression induced by the protein kinase C and tyrosine
516 kinase pathways in cultured human thyroid follicles. *The Journal of Clinical*
517 *Endocrinology and Metabolism*, 82(6), 1839–1844.
518 <https://doi.org/10.1210/jcem.82.6.4024>
- 519 Hoa, N. K., Norberg, A., Sillard, R., Van Phan, D., Thuan, N. D., Dzung, D. T. N.,
520 Jornvall, H., & Ostenson, C.-G. (2007). The possible mechanisms by which
521 phanoside stimulates insulin secretion from rat islets. *Journal of Endocrinology*,
522 192(2), 389–394. <https://doi.org/10.1677/joe.1.06948>
- 523 Hur, K. C. (2005). Protein Kinase a functions as a negative regulator of c-jun
524 n-terminal kinase but not of p38 mitogen-activated protein Kinase in PC12 cells.

- 525 *Integrative Biosciences*, 9(3), 173–179.
- 526 <https://doi.org/10.1080/17386357.2005.9647268>
- 527 Huyen, V. T. T., Phan, D. V., Thang, P., Hoa, N. K., & Östenson, C. G. (2013).
- 528 Gynostemma pentaphyllum Tea Improves Insulin Sensitivity in Type 2 Diabetic
- 529 Patients. *Journal of Nutrition and Metabolism*, 2013.
- 530 <https://doi.org/10.1155/2013/765383>
- 531 Huyen, V. T. T., Phan, D. V., Thang, P., Ky, P. T., Hoa, N. K., & Ostenson, C. G.
- 532 (2012). Antidiabetic Effects of Add-On Gynostemma pentaphyllum Extract
- 533 Therapy with Sulfonylureas in Type 2 Diabetic Patients. *Evidence-Based*
- 534 *Complementary and Alternative Medicine*, 2012, 452313.
- 535 <https://doi.org/10.1155/2012/452313>
- 536 Iwamoto, T. (2004). Forefront of Na⁺/Ca²⁺ exchanger studies: molecular
- 537 pharmacology of Na⁺/Ca²⁺ exchange inhibitors. *Journal of Pharmacological*
- 538 *Sciences*, 96(1), 27–32. <https://doi.org/10.1254/jphs.FMJ04002X6>
- 539 Jiang, W., Peng, Y., & Yang, K. (2018). Cellular signaling pathways regulating β cell
- 540 proliferation as a promising therapeutic target in the treatment of diabetes
- 541 (Review). *Experimental and Therapeutic Medicine*, 16(4), 3275–3285.
- 542 <https://doi.org/10.3892/etm.2018.6603>
- 543 Karaskov, E., Scott, C., Zhang, L., Teodoro, T., Ravazzola, M., & Volchuk, A. (2006).
- 544 Chronic palmitate but not oleate exposure induces endoplasmic reticulum
- 545 stress, which may contribute to INS-1 pancreatic beta-cell apoptosis.
- 546 *Endocrinology*, 147(7), 3398–3407. <https://doi.org/10.1210/en.2005-1494>
- 547 Kiely, A., McClenaghan, N. H., Flatt, P. R., & Newsholme, P. (2007).
- 548 Proinflammatory cytokines increase glucose, alanine and triacylglycerol
- 549 utilization but inhibit insulin secretion in a clonal pancreatic beta-cell line. *The*

- 550 *Journal of Endocrinology*, 195(1), 113–123. <https://doi.org/10.1677/JOE-07->
551 0306
- 552 Kim, J. W., Roberts, C. D., Berg, S. A., Caicedo, A., & Roper, S. D. (2008). Imaging
553 Cyclic AMP Changes in Pancreatic Islets of Transgenic Reporter Mice. *PLoS*
554 *ONE*, 3(5), 2127. <https://doi.org/10.1371/journal.pone.0002127>
- 555 Kulkarni, S. R., Donepudi, A. C., Xu, J., Wei, W., Cheng, Q. C., Driscoll, M. V.,
556 Johnson, D. A., Johnson, J. A., Li, X., & Slitt, A. L. (2014). Fasting induces
557 nuclear factor E2-related factor 2 and ATP-binding Cassette transporters via
558 protein kinase A and Sirtuin-1 in mouse and human. *Antioxidants & Redox*
559 *Signaling*, 20(1), 15–30. <https://doi.org/10.1089/ars.2012.5082>
- 560 Li, L., Jiao, L., & Lau, B. H. (1993). Protective effect of gypenosides against oxidative
561 stress in phagocytes, vascular endothelial cells and liver microsomes. *Cancer*
562 *Biotherapy*, 8(3), 263–272. <https://doi.org/10.1089/cbr.1993.8.263>
- 563 Lokman, E. F., Gu, H. F., Wan Mohamud, W. N., & Östenson, C.-G. (2015).
564 Evaluation of Antidiabetic Effects of the Traditional Medicinal Plant *Gynostemma*
565 *pentaphyllum* and the Possible Mechanisms of Insulin Release. *Evidence-Based*
566 *Complementary and Alternative Medicine*, 2015, 1–7.
567 <https://doi.org/10.1155/2015/120572>
- 568 Lupi, R., Dotta, F., Marselli, L., Del Guerra, S., Masini, M., Santangelo, C., Patané,
569 G., Boggi, U., Piro, S., Anello, M., Bergamini, E., Mosca, F., Di Mario, U., Del
570 Prato, S., & Marchetti, P. (2002). Prolonged exposure to free fatty acids has
571 cytostatic and pro-apoptotic effects on human pancreatic islets: evidence that
572 beta-cell death is caspase mediated, partially dependent on ceramide pathway,
573 and Bcl-2 regulated. *Diabetes*, 51(5), 1437–1442.
574 <https://doi.org/10.2337/diabetes.51.5.1437>

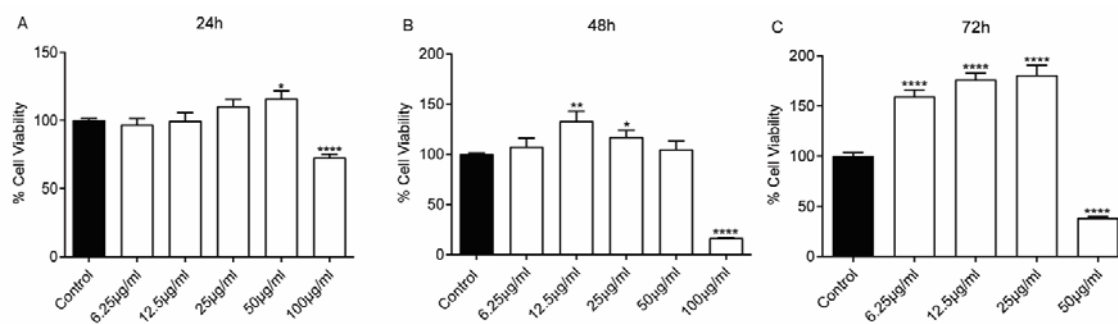
- 575 Lytton, J., Westlin, M., & Hanley, M. R. (1991). Thapsigargin inhibits the
576 sarcoplasmic or endoplasmic reticulum Ca-ATPase family of calcium pumps.
577 *The Journal of Biological Chemistry*, 266(26), 17067–17071.
578 <http://www.ncbi.nlm.nih.gov/pubmed/1832668>
- 579 Mancini, A. D., & Poitout, V. (2013). The fatty acid receptor FFA1/GPR40 a decade
580 later: how much do we know? *Trends in Endocrinology & Metabolism*, 24(8),
581 398–407. <https://doi.org/10.1016/j.tem.2013.03.003>
- 582 Masuda, Y., Vaziri, N. D., Li, S., Le, A., Hajighasemi-Ossareh, M., Robles, L., Foster,
583 C. E., Stamos, M. J., Al-Abodullah, I., Ricordi, C., & Ichii, H. (2015). The effect of
584 Nrf2 pathway activation on human pancreatic islet cells. *PloS One*, 10(6),
585 e0131012. <https://doi.org/10.1371/journal.pone.0131012>
- 586 Megalli, S., Davies, N. M., & Roufogalis, B. D. (2006). Anti-hyperlipidemic and
587 hypoglycemic effects of *Gynostemma pentaphyllum* in the Zucker fatty rat.
588 *Journal of Pharmacy & Pharmaceutical Sciences*, 9(3), 281–291.
589 <http://www.ncbi.nlm.nih.gov/pubmed/17207412>
- 590 Melloul, D., Marshak, S., & Cerasi, E. (2002). Regulation of insulin gene
591 transcription. *Diabetologia*, 45(3), 309–326. [https://doi.org/10.1007/s00125-001-](https://doi.org/10.1007/s00125-001-0728-y)
592 [0728-y](https://doi.org/10.1007/s00125-001-0728-y)
- 593 Meng, X., Wang, M., Sun, G., Ye, J., Zhou, Y., Dong, X., Wang, T., Lu, S., & Sun, X.
594 (2014). Attenuation of A β 25-35-induced parallel autophagic and apoptotic cell
595 death by gypenoside XVII through the estrogen receptor-dependent activation of
596 Nrf2/ARE pathways. *Toxicology and Applied Pharmacology*, 279(1), 63–75.
597 <https://doi.org/10.1016/j.taap.2014.03.026>
- 598 Müller, C., Gardemann, A., Keilhoff, G., Peter, D., Wiswedel, I., & Schild, L. (2012).
599 Prevention of free fatty acid-induced lipid accumulation, oxidative stress, and

- 600 cell death in primary hepatocyte cultures by a *Gynostemma pentaphyllum*
601 extract. *Phytomedicine*, 19(5), 395–401.
602 <https://doi.org/10.1016/j.phymed.2011.12.002>
- 603 Newsholme, P., & Krause, M. (2012). Nutritional regulation of insulin secretion:
604 implications for diabetes. *The Clinical Biochemist. Reviews*, 33(2), 35–47.
605 <http://www.ncbi.nlm.nih.gov/pubmed/22896743>
- 606 Oh, Y. S., Bae, G. D., Baek, D. J., Park, E.-Y., & Jun, H.-S. (2018). Fatty Acid-
607 Induced Lipotoxicity in Pancreatic Beta-Cells During Development of Type 2
608 Diabetes. *Frontiers in Endocrinology*, 9.
609 <https://doi.org/10.3389/fendo.2018.00384>
- 610 Padmanabhan, A., Li, X., & Bieberich, C. J. (2013). Protein Kinase A Regulates MYC
611 Protein through Transcriptional and Post-translational Mechanisms in a Catalytic
612 Subunit Isoform-specific Manner. *Journal of Biological Chemistry*, 288(20),
613 14158–14169. <https://doi.org/10.1074/jbc.M112.432377>
- 614 Philipson, K. D., Nicoll, D. A., Ottolia, M., Quednau, B. D., Reuter, H., John, S., &
615 Qiu, Z. (2002). The Na⁺/Ca²⁺ exchange molecule: an overview. *Annals of the*
616 *New York Academy of Sciences*, 976, 1–10. [https://doi.org/10.1111/j.1749-](https://doi.org/10.1111/j.1749-6632.2002.tb04708.x)
617 [6632.2002.tb04708.x](https://doi.org/10.1111/j.1749-6632.2002.tb04708.x)
- 618 Puri, S., Roy, N., Russ, H. A., Leonhardt, L., French, E. K., Roy, R., Bengtsson, H.,
619 Scott, D. K., Stewart, A. F., & Hebrok, M. (2018). Replication confers β cell
620 immaturity. *Nature Communications*, 9(1), 485. [https://doi.org/10.1038/s41467-](https://doi.org/10.1038/s41467-018-02939-0)
621 [018-02939-0](https://doi.org/10.1038/s41467-018-02939-0)
- 622 Quan, W., Jo, E.-K., & Lee, M.-S. (2013). Role of pancreatic β -cell death and
623 inflammation in diabetes. *Diabetes, Obesity & Metabolism*, 15(s3), 141–151.
624 <https://doi.org/10.1111/dom.12153>

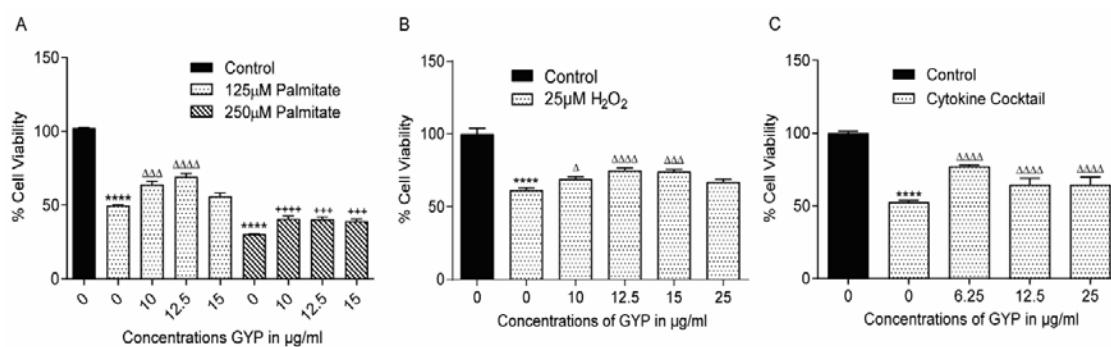
- 625 Sharp, G. W., Wiedenkeller, D. E., Kaelin, D., Siegel, E. G., & Wollheim, C. B.
626 (1980). Stimulation of adenylate cyclase by Ca²⁺ and calmodulin in rat islets of
627 langerhans: explanation for the glucose-induced increase in cyclic AMP levels.
628 *Diabetes*, 29(1), 74–77. <https://doi.org/10.2337/diab.29.1.74>
- 629 Sivitz, W. I., & Yorek, M. A. (2010). Mitochondrial dysfunction in diabetes: from
630 molecular mechanisms to functional significance and therapeutic opportunities.
631 *Antioxidants & Redox Signaling*, 12(4), 537–577.
632 <https://doi.org/10.1089/ars.2009.2531>
- 633 Takahashi, N., Tetsuka, T., Uranishi, H., & Okamoto, T. (2002). Inhibition of the NF-
634 kappaB transcriptional activity by protein kinase A. *European Journal of*
635 *Biochemistry*, 269(18), 4559–4565. [https://doi.org/10.1046/j.1432-](https://doi.org/10.1046/j.1432-1033.2002.03157.x)
636 [1033.2002.03157.x](https://doi.org/10.1046/j.1432-1033.2002.03157.x)
- 637 Tiedge, M., Lortz, S., Drinkgern, J., & Lenzen, S. (1997). Relation between
638 antioxidant enzyme gene expression and antioxidative defense status of insulin-
639 producing cells. *Diabetes*, 46(11), 1733–1742.
640 <https://doi.org/10.2337/diab.46.11.1733>
- 641 Van Eylen, F, Svoboda, M., & Herchuelz, A. (1997). Identification, expression pattern
642 and potential activity of Na/Ca exchanger isoforms in rat pancreatic B-cells. *Cell*
643 *Calcium*, 21(3), 185–193. [https://doi.org/10.1016/S0143-4160\(97\)90043-9](https://doi.org/10.1016/S0143-4160(97)90043-9)
- 644 Van Eylen, Françoise, Horta, O. D., Barez, A., Kamagate, A., Flatt, P. R.,
645 Macianskiene, R., Mubagwa, K., & Herchuelz, A. (2002). Overexpression of the
646 Na/Ca exchanger shapes stimulus-induced cytosolic Ca²⁺ oscillations in
647 insulin-producing BRIN-BD11 cells. *Diabetes*, 51(2), 366–375.
648 <https://doi.org/10.2337/diabetes.51.2.366>
- 649 Vasu, S., McClenaghan, N. H., McCluskey, J. T., & Flatt, P. R. (2014). Mechanisms

- 650 of toxicity by proinflammatory cytokines in a novel human pancreatic beta cell
651 line, 1.1B4. *Biochimica et Biophysica Acta*, 1840(1), 136–145.
652 <https://doi.org/10.1016/j.bbagen.2013.08.022>
- 653 Wan, Z.-H., & Zhao, Q. (2017). Gypenoside inhibits interleukin-1 β -induced
654 inflammatory response in human osteoarthritis chondrocytes. *Journal of*
655 *Biochemical and Molecular Toxicology*, 31(9), e21926.
656 <https://doi.org/10.1002/jbt.21926>
- 657 Wang, J., & Wang, H. (2017). Oxidative Stress in Pancreatic Beta Cell Regeneration.
658 *Oxidative Medicine and Cellular Longevity*, 2017, Article ID 1930261.
659 <https://doi.org/10.1155/2017/1930261>
- 660 Wang, R., McGrath, B. C., Kopp, R. F., Roe, M. W., Tang, X., Chen, G., & Cavener,
661 D. R. (2013). Insulin Secretion and Ca²⁺ Dynamics in β -Cells Are Regulated by
662 PERK (EIF2AK3) in Concert with Calcineurin. *Journal of Biological Chemistry*,
663 288(47), 33824–33836. <https://doi.org/10.1074/jbc.M113.503664>
- 664 Yagishita, Y., Fukutomi, T., Sugawara, A., Kawamura, H., Takahashi, T., Pi, J.,
665 Uruno, A., & Yamamoto, M. (2014). Nrf2 protects pancreatic β -cells from
666 oxidative and nitrosative stress in diabetic model mice. *Diabetes*, 63(2), 605–
667 618. <https://doi.org/10.2337/db13-0909>
- 668 Yang, S.-N., & Berggren, P.-O. (2006). The role of voltage-gated calcium channels in
669 pancreatic beta-cell physiology and pathophysiology. *Endocrine Reviews*, 27(6),
670 621–676. <https://doi.org/10.1210/er.2005-0888>
- 671 Yassin, K., Huyen, V. T. T., Hoa, K. N., & Ostenson, C. G. (2011). Herbal extract of
672 gynostemma pentaphyllum decreases hepatic glucose output in type 2 diabetic
673 goto-kakizaki rats. *International Journal of Biomedical Science*, 7(2), 131–136.
674 <http://www.ncbi.nlm.nih.gov/pubmed/23675229>

675 Zhang, C., Moriguchi, T., Kajihara, M., Esaki, R., Harada, A., Shimohata, H., Oishi,
676 H., Hamada, M., Morito, N., Hasegawa, K., Kudo, T., Engel, J. D., Yamamoto,
677 M., & Takahashi, S. (2005). MafA is a key regulator of glucose-stimulated insulin
678 secretion. *Molecular and Cellular Biology*, 25(12), 4969–4976.
679 <https://doi.org/10.1128/MCB.25.12.4969-4976.2005>

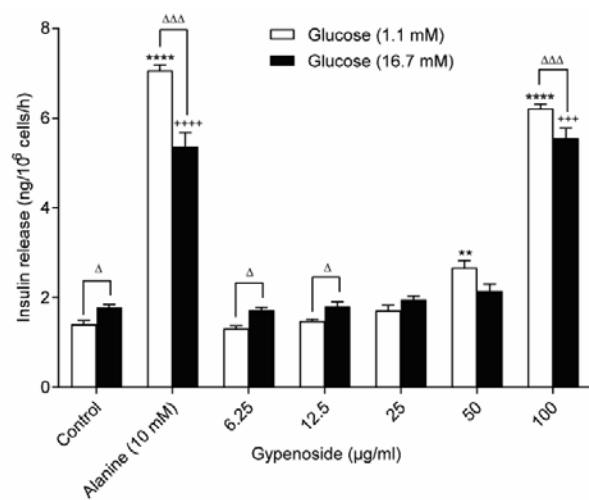


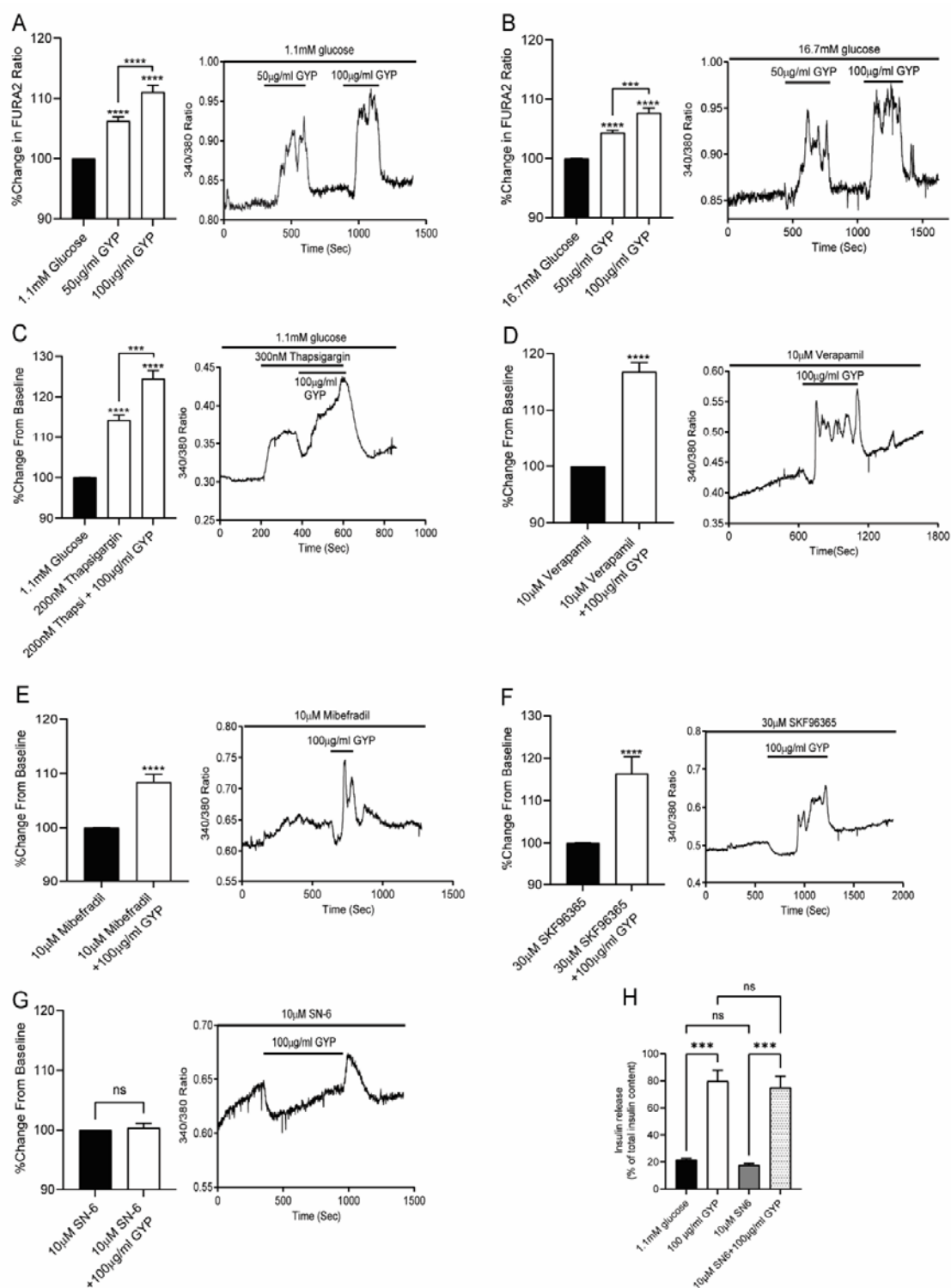
680 **Figure 1**



681 **Figure 2**

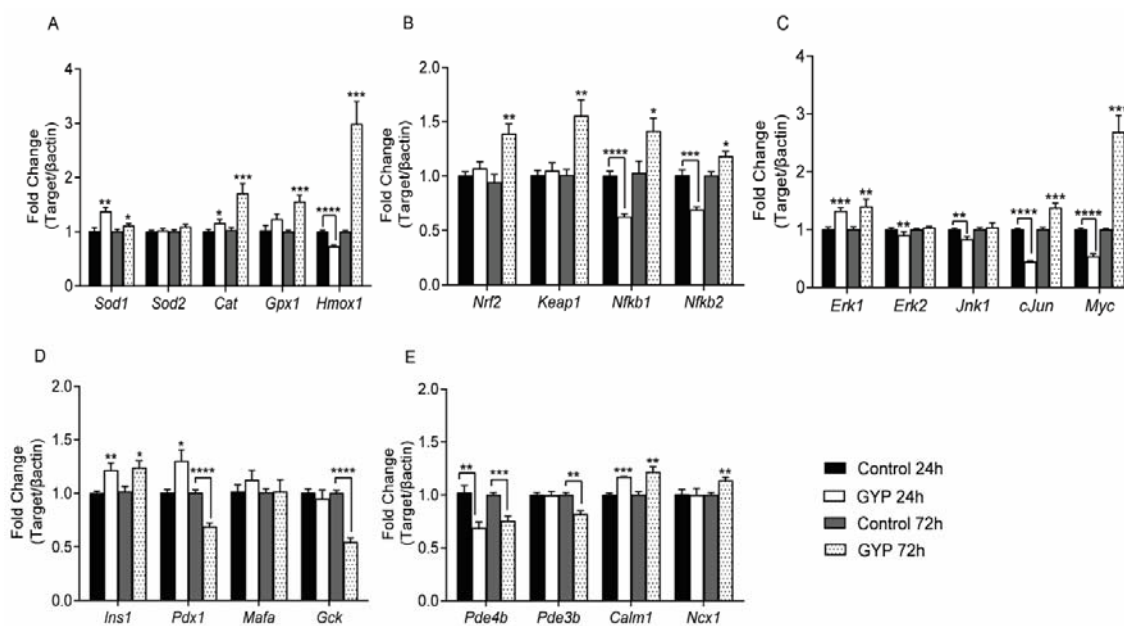
682 **Figure 3**



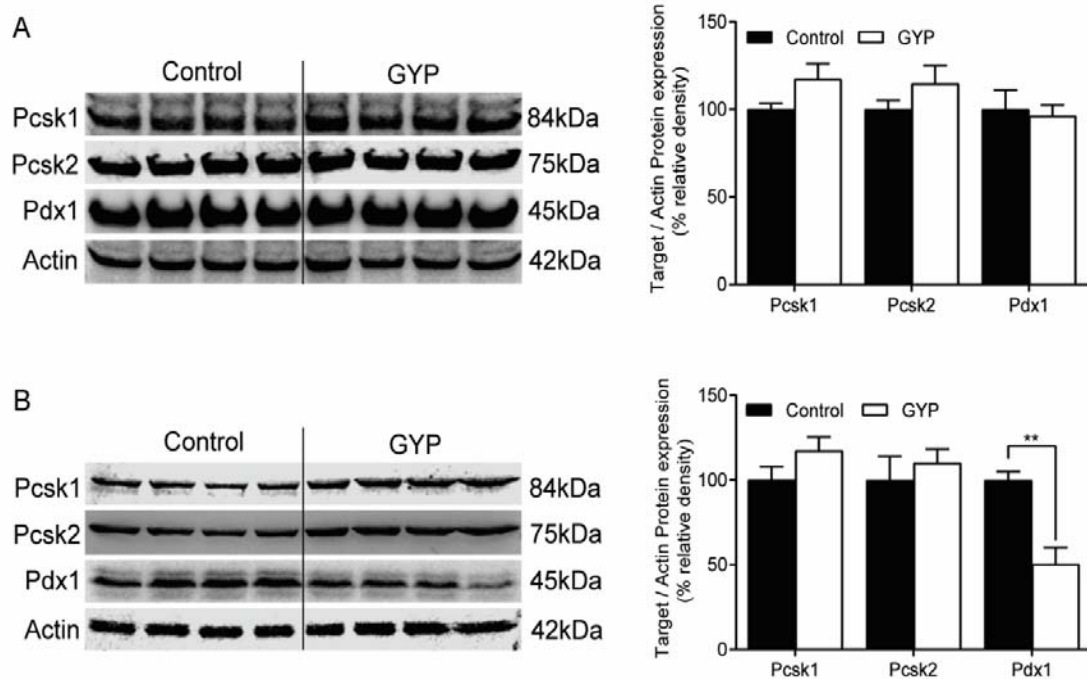


683 **Figure 4**

684 **Figure 5**



685 **Figure 6**



686 **Figure Legends:**

687 **Figure 1:** Effects of GYP addition to BRIN-BD11 cell culture medium at
688 concentrations between 6.25–100 µg/ml on cell viability following 24h (A), 48 h (B),
689 and 72h (C) treatment. Plotted as % change in cell viability compared to
690 control. Values represent mean ±S.E.M. from three different experiments (n=4). The
691 student's t-test was used for statistical analysis. *P<0.05; **P<0.01; ****P<0.0001,
692 compared to control (no GYP addition).

693 **Figure 2:** Protective effects of GYP against detrimental effects of palmitate (A),
694 peroxide (B), and cytokine cocktail (C) on BRIN-BD11 cell viability. Cells were
695 cultured with palmitate and GYP for 24 h prior to cell viability measurement by MTT
696 assay. For H₂O₂, cells were exposed to treatment for 6h alone or in combination with
697 GYP. For cytokine treatment, cells were exposed to a cytokine cocktail containing IL-
698 1β (50U), TNF-α (1000U), and IFN-γ (1000U) for 24 h either alone or in combination
699 with GYP. Values represent mean ±S.E.M. from three different experiments (n=4).
700 The student's t-test was used for statistical analysis. ****P<0.0001 compared to
701 control (black bar); ^ΔP<0.05, ^{ΔΔ}P<0.001, ^{ΔΔΔ}P<0.0001 compared to 125 µM
702 palmitate, H₂O₂ or cytokine cocktail treatment alone. ; ⁺⁺⁺P<0.001; ⁺⁺⁺⁺P<0.0001
703 compared to 250 µM palmitate alone.

704 **Figure 3:** Concentration-dependent effects of gypenosides on insulin secretion from
705 BRIN-BD11 cells. Insulin secretion measured in presence of GYP 6.25 - 100µg/ml at
706 low (1.1mM) (white bars) or high (16.7mM) (black bars) glucose concentrations. Data
707 plotted as concentration of insulin secreted in ng/10⁶ cells per h. Values plotted as
708 mean ± S.E.M. from 4 independent experiments conducted in duplicate. **P<0.01,
709 ****P<0.0001 compared to 1.1 mM glucose control; ^ΔP<0.05, ^{ΔΔ}P<0.001 compared

710 to respective 1.1 mM glucose result; $^{***}P<0.001$, $^{****}P<0.0001$ compared to 16.7
711 mM glucose control.

712 **Figure 4:** Effects of GYP on intracellular Ca^{2+} levels of BRIN-BD11 cells alone and
713 in the presence of specific calcium channel modulators. Graphs showing the %
714 change in FURA2 ratio (340/380) from baseline over time (left) and representative
715 plot (right) when perfused with GYP in the presence of low (1.1 mM) (A) and high
716 (16.7 mM) (B) glucose concentrations, Thapsigargin (C), L-type calcium channel
717 blocker verapamil (D), T-type calcium channel blocker Mibefradil (E) SOCC blocker
718 SKF96365 (F) and NCX channel reverse mode inhibitor SN-6 (G). Values plotted as
719 mean responses of 3-15 responding cells from three independent experiments—
720 Effects of SN-6 on GYP induced insulin secretion in 1.1mM glucose (H). Data plotted
721 as % of insulin secreted from total content. Values plotted as mean \pm S.E.M. from 3
722 independent experiments. $^{***}P<0.001$, $^{****}P<0.0001$.

723 **Figure 5:** Effects of 24 and 72 h culture with GYP (12.5 μ g/ml) on the expression of
724 antioxidant and β cell-specific genes in BRIN-BD11 cells. Data represent fold-change
725 in mRNA levels compared to control/untreated BRIN-BD11 cell and normalised to β -
726 actin expression. Values represent mean \pm S.E.M. from three different experiments
727 performed in duplicate. $^{*}P<0.05$, $^{**}P<0.01$, $^{***}P<0.001$, $^{****}P<0.0001$ compared to
728 their respective 24h or 72h control.

729 **Figure 6:** Effects of GYP (12.5 μ g/ml) treatment for 24 h (A, B) and 72 h (C, D) on
730 the expression of Pdx1 and prohormone convertases 1 and 2 in BRIN-BD11
731 cells. Protein levels for each treatment were normalised to Actin expression, plotted
732 as % change relative to control. Values represent mean \pm S.E.M. from four different
733 experiments. $^{**}P<0.01$ compared to respective control.